Tunable Nanometer Electrode Gaps by MeV Ion Irradiation

Tunable nanometer electrode gaps by MeV ion irradiation

J.-C. Cheang-Wong,[1,a)] K. Narumi,[1,b)] G.M. Schürmann,[1,c)] M. J. Aziz,[2] and J. A. Golovchenko[1,2,d)]

[1]Department of Physics, Harvard University, Cambridge, MA, 02138, USA

[2]School of Engineering and Applied Sciences, Harvard University, Cambridge, MA, 02138, USA

We report the use of MeV ion-irradiation-induced plastic deformation of amorphous materials to fabricate electrodes with nanometer-sized gaps. Plastic deformation of the amorphous metal $Pd_{80}Si_{20}$ is induced by 4.64 MeV O^{2+} ion irradiation, allowing the complete closing of a sub-micrometer gap. We measure the evolving gap size *in situ* by monitoring the field emission current-voltage (*I*-*V*) characteristics between electrodes. The *I*-*V* behavior is consistent with Fowler-Nordheim tunneling. We show that using feedback control on this signal permits gap size fabrication with atomic-scale precision. We expect this approach to nanogap fabrication will enable the practical realization of single molecule controlled devices and sensors.

---

a)Current Address: Instituto de Física, Universidad Nacional Autónoma de México. A.P. 20-364, México D.F., 01000, Mexico.

b)Current Address: Takasaki Advanced Radiation Research Institute, Japan Atomic Energy Agency, Takasaki 370-1292, Japan.

c)Current Address: Robert Bosch GmbH, Sensor Technology Center (AE/EST2), 72703 Reutlingen, Germany

d)Author to whom correspondence should be addressed. Electronic mail: golovchenko@physics.harvard.edu

In nanostructure fabrication, it is often a challenge to precisely control and characterize critical dimensions, such as the size of a gap between two metallic electrodes. Such a structure is fundamental for nanoscale electronic devices, including those with small molecules in the gap that may become essential components of future devices, and long molecules such as DNA that may lend themselves to extremely rapid sequencing through their electrical signals[1]. A variety of methods has been used for the fabrication of electrodes with a nanometer-sized gap: mechanical break junctions[2], electron-beam deposition[3], oblique evaporation through a lift-off mask[4], electrochemical deposition[5,6], electromigration[7], electron-beam lithography[8,9], and focused-ion-beam lithography[10]. With some of these methods, the gap has been controlled by measuring the electrical properties of electrodes *in situ*[2, 4-6].

Amorphous materials, such as SiO_2 or $Pd_{80}Si_{20}$, are known to be deformed plastically by MeV ion irradiation[11-14]. The electronic energy loss of the incoming MeV ions causes an anisotropic deformation consisting of an increase in the sample dimensions perpendicular to the ion beam and a decrease in the dimension parallel to the ion beam[15]. Induced strains accumulate with increasing ion beam fluence and can exceed unity, causing microns of dimensional changes. Hence, the phenomenon can be used for precise nanostructure fabrication if *in situ* feedback control can be implemented based on some physical quantity such as a tunneling current reflecting a critical dimension.

In this Letter, we demonstrate that we can fabricate amorphous metallic $Pd_{80}Si_{20}$ electrodes with a nanometer-sized gap by using MeV oxygen ion irradiation-induced plastic

deformation. We also demonstrate that the gap size can be controlled with nanometer precision by *in situ* feedback control using the field-emission current between the electrodes.

We prepared a layered $Pd_{80}Si_{20}/SiO_2/Si$ structure with an H-shaped trench, as shown in Fig. 1. A 500 nm thick SiO_2 layer was grown by thermal oxidation of a Si substrate and then a 200 nm-thick $Pd_{80}Si_{20}$ film was deposited by Ar^+ ion beam sputtering from a target of the same composition. The H-shaped trench was micromachined using a 50 keV Ga^+ beam from a Micrion 9500 Focused Ion Beam instrument. The trench width was ~800 nm. The milled depth was ~1.1 μm, so that the lower part of the side walls visible in Fig. 1(a) corresponds to the silicon substrate. Irradiation at normal incidence with 4.64 MeV O^{2+} ions was performed either at room temperature (RT) or at liquid nitrogen temperature (~80 K) with the use of a General Ionex 1.7 MV tandem accelerator. The beam spot was 1 mm in diameter and the beam current was typically ~6 nA. The pressure in the irradiation chamber was roughly 10^{-5} Pa. The energy of the incident oxygen ions was high enough to allow the ions to penetrate through the $Pd_{80}Si_{20}/SiO_2$ bilayer and come to rest within the Si substrate[16]. Every sample was characterized before and after irradiation by using scanning electron microscopy (SEM). Moreover, the cross section of some samples was studied with atomic force microscopy (AFM).

Figure 1(b) shows an SEM image of the sample irradiated with 1×10^{16} ions/cm^2 at RT. Plastic deformation due to the ion irradiation was observed in both $Pd_{80}Si_{20}$ and SiO_2 layers. The walls surrounding the gap deform into the gap in all directions. The SiO_2 walls become especially quite rounded and are almost in contact, indicating that the SiO_2 deformation rate is larger than that of $Pd_{80}Si_{20}$ under these conditions. We observed no dimensional modification to

the crystalline silicon substrate from this treatment. From SEM images, we evaluated and compared the relative width change of the gap of $Pd_{80}Si_{20}$ and SiO_2 in the bilayered structure as a function of the irradiation fluence. Figure 2 shows a comparison of the width changes for irradiations at RT and 80 K. At RT and 80 K, SiO_2 deforms almost three times and about two times as much, respectively, as does $Pd_{80}Si_{20}$. In all cases, the gap width decreases almost linearly with ion fluence. Moreover, low temperature irradiation induces more significant deformations of $Pd_{80}Si_{20}$ and SiO_2 compared with those obtained at RT. We have previously demonstrated that this kind of deformation does not occur in the case of a crystalline pure metal (Al, Au) on top of a similar SiO_2 layer[17].

From Fig. 2 it is apparent that, at least for RT irradiations, the $Pd_{80}Si_{20}$ gap width saturates once the SiO_2 gap is closed. This result indicates that the $Pd_{80}Si_{20}$ gap closure is restrained by the complete closure of the underlying SiO_2 gap (see Fig. 1(b)). To eliminate this restraint, we dipped the irradiated sample in a H_2O:HF = 10:1 solution, which removed the SiO_2 underneath the $Pd_{80}Si_{20}$ gap. In Fig. 1(c) is the SEM image of the same sample from Fig. 1(b) after it has been etched in diluted HF for 4 minutes. The SiO_2 gap is open again up to the same width as the silicon gap (800 nm), and the etched SiO_2 gap is wider than that of the $Pd_{80}Si_{20}$ (~500 nm), which is not affected by the etching. Next, we chose a second irradiation treatment under conditions expected to completely close the gap based on the data in Fig. 2: 1×10^{16} ions/cm^2 at 80 K. Figure 1(d) shows an SEM image of the resulting sample. Not only has the $Pd_{80}Si_{20}$ gap been completely closed, but also the deformation of the free-standing portion of the $Pd_{80}Si_{20}$ layers has been large enough to cause buckling.

For controlling the gap separation with nanometer precision, we prepared another type of sample: a layered structure of $Si_3N_4/SiO_2/Si$ with $Pd_{80}Si_{20}$ electrodes, as illustrated in Fig. 3(a). A 200 nm thick Si_3N_4 film was grown by chemical vapor deposition on a 500 nm thick SiO_2 layer grown by thermal oxidation of a Si wafer. A $Pd_{80}Si_{20}$ line, 100 nm thick and 3 μm wide, was prepared by Ar^+ ion beam sputtering, photolithography and lift-off techniques. Then the line was cut using the FIB. In order to minimize the influence of the underlying SiO_2 layer on the deformation of the $Pd_{80}Si_{20}$ electrodes, the SiO_2 layer was etched in a buffered HF solution for 3.5 minutes and then in a H_2O:HF = 50:1 solution for 5 minutes. Figure 3(b) shows an SEM image of the electrodes displaying a gap of about 130 nm.

We monitored the I-V characteristics of the pair of electrodes during O^{2+} irradiation at RT. The ion irradiation was paused between incremental ion doses while I-V behavior was characterized over a series of ion irradiation fluences. The results for the series are shown in Fig. 4. Each curve shows the characteristics of field emission, and the abrupt current rise shifts to lower voltage with increasing ion irradiation fluence. These results indicate that the change in the I-V characteristics with fluence reflects a continuous shrinkage of the electrode separation with increasing fluence. This interpretation is confirmed by Fig. 3(c), taken after the final irradiation fluence in Fig. 4 and showing that the gap between the $Pd_{80}Si_{20}$ electrodes is almost completely closed after an irradiation with 5.65×10^{15} ions/cm^2 at RT. Although Fig. 3(c) indicates that the Si_3N_4 layer has been deformed in addition to the $Pd_{80}Si_{20}$ layer, detailed SEM observations not reproduced here confirmed that the gap between the Si_3N_4 layers was still open after this fluence.

According to elementary Fowler-Nordheim theory[18,19], the relation between the emission current I and the applied voltage V can be written in the following logarithmic form:

$$\ln\frac{I}{V^2} = \ln\left[\frac{e^3}{16\pi^2\hbar\phi}\frac{S}{L^2}\right] - \frac{4\sqrt{2m}}{3e\hbar}\phi^{3/2}\frac{L}{V}\ , \qquad (1)$$

where e is the elementary positive charge, m is the electron mass, $\hbar$ is the Planck's constant divided by 2π, ϕ is the work function, S is the emission area and L is the gap. In this equation, the exchange-and-correlation interaction between the emitted electron and the surface is neglected and a simple triangular barrier (i.e., spatially uniform field near the emitter tip) is assumed. According to Equation 1, for field emission, a "F-N plot" of $\ln(I/V^2)$ vs. $1/V$ should exhibit linear behavior. The F-N plots of our data (not reproduced here) yielded nearly straight lines. A linear least-squares fit of $\ln(I/V^2)$ vs. $1/V$ yielded parameters used to construct the (nonlinear) dashed curves superposed on the data in Fig. 4. The good agreement illustrated in Fig. 4 indicates that the observed I-V characteristics can be attributed to field emission. Although the three variables (S, L, ϕ) appear in Equation (1) in only two combinations, ($S/(\phi L^2)$) and ($L\phi^{3/2}$), we identify unique values of all three variables as described below. The coefficient of $1/V$ in Equation (1) depends on both L and ϕ; however, we presume that the fluence dependence of the coefficient of $1/V$, i.e., the slope of the line in the F-N plot, reflects a change only in the gap distance because we presume the work function of $Pd_{80}Si_{20}$ is not changed by MeV ion irradiation (after, perhaps, an initial transient). When plotted as a function of the fluence, the coefficient of $1/V$ in Equation (1) increases linearly with irradiation fluence and is almost zero at 5.65×10^{15} ions/cm^2 (not shown). This is consistent with the result shown in Fig. 2 that the gap width decreases almost

linearly with ion fluence, and supports our presumption. Thus, if we once determine by any means a value of ϕ at any particular value of L, we can uniquely determine the three variables (S, L, ϕ) at any irradiation fluence. We did not obtain any experimental value of L during the experiment reported in Fig. 4. However, in a similar experiment with a known gap distance of 10 nm, the I-V characteristic fit Equation (1) with $\phi = 5.7$ eV. Assuming ϕ does not vary from sample to sample permits us to apply this value to the data in Fig. 4 and thereby uniquely determine all three parameters.

The quantitative analysis of tunneling I-V curves permits exquisite measurement and control of gap dimensions. The typical increment of irradiation fluence in the present experiment is 6×10^{13} ions/cm^2, which corresponds to a 1.2 nm decrease in gap distance. The scatter in the data and the quality of the fit are sufficiently good that cutting the fluence increment by a factor of six, to 1×10^{13} ions/cm^2, corresponding to gap changes of 0.2 nm, should result in distinguishable *I-V* curves - especially for the smallest gaps. Hence we believe that these results demonstrate fabrication precision at the scale of the diameter of an individual atom.

Acknowledgments

J.C. Ch.-W. was supported by DGAPA-UNAM and CONACYT (Mexico) during his sabbatical leave at Harvard University. K.N. was supported by the Japanese Ministry of Education, Culture, Sports, Science and Technology during his stay in Harvard University. The research of M.J.A. was supported by the U.S. DOE, Office of Basic Energy Sciences, Division of Materials Sciences and Engineering under Award # DE-FG02-06 ER46335. The research of J.A.G. was supported by the National Institutes of Health Award #R01HG003703. The authors are grateful to Mr. J.F. Chervinsky for operating the accelerator, to Dr. V. Ramaswamy and Dr. A. Donohue for helping with sample preparation and to Dr. T. Mitsui for performing electrical measurements. The ion beam instruments are operated by the Center for Nanoscale Systems at Harvard University.

Author Contributions

All of the authors designed the experiments and analyzed the data. J.C. Ch.-W., K.N., and G.M.S. performed the experiments. All authors discussed the results.

References

[1]J. Li, M. Gershow, D. Stein, E. Brandin, and J. Golovchenko, Nature Materials **2**, 611 (2003).

[2]M.A. Reed, C. Zhou, C.J. Muller, T.P. Burgin, and J.M. Tour, Science **278**, 252 (1997).

[3]A. Bezryadin and C.J. Dekker, J. Vac. Sci. Technol. B **15**, 793 (1997).

[4]S.E. Kubatkin, A.V. Danilov, A.L. Bogdanov, H. Olin, and T. Claeson, Appl. Phys. Lett. **73**, 3604 (1998).

[5]A.F. Morpurgo, C.M. Marcus, and D.B. Robinson, Appl. Phys. Lett. **74**, 2084 (1999).

[6]Y.V. Kervennic, H.S.J. Van der Zant, A.F. Morpurgo, L. Gurevich, and L.P. Kouwenhoven, Appl. Phys. Lett. **80**, 321 (2002).

[7]H. Park, A.K.L. Lim, A.P. Alivisatos, J. Park, and P.L. McEuen, Appl. Phys. Lett. **75**, 301 (1999).

[8]M.A. Guillorn, D.W. Carr, R.C. Tiberio, E. Greenbaum, and M.L. Simpson, J. Vac. Sci. Technol. B **18**, 1177 (2000).

[9]K. Liu, Ph. Avouris, J. Bucchignano, R. Martel, S. Sun, and J. Michi., Appl. Phys. Lett. **80**, 865 (2002).

[10]T. Nagase, T. Kubota, and S. Mashiko, Thin Solid Films **438-439**, 374 (2003).

[11]Md. Hou, S. Klaumünzer, and G. Schumacher, Phys. Rev. B Condens. Matter **41**, 1144 (1990).

[12]M.L. Brongersma, E. Snoeks, T. van Dillen, and A. Polman, J. Appl. Phys. **88**, 59 (2000).

[13]J.C. Cheang-Wong, U. Morales, A. Oliver, L. Rodríguez-Fernández, and J. Rickards, Nucl. Instr. and Meth. B **242**, 452 (2006).

[14]H.B. George, D.P. Hoogerheide, C.S. Madi, D.C. Bell, J.A. Golovchenko, and M.J. Aziz, Appl. Phys. Lett. **96**, 263111 (2010).

[15]T. van Dillen, A. Polman, P.R. Onck, and E. van der Giessen, Physical Review B **71**, 024103 (2005).

[16]J.F. Ziegler, J.P. Biersack, and U. Littmark, *The stopping and range of ions in solids* (Pergamon, New York, 1985).

[17]J.C. Cheang-Wong, Rad. Eff. & Def. in Solids **162**, 247 (2007).

[18]R.H. Fowler and L. Nordheim, Proc. R. Soc. London A **119**, 173 (1928).

[19] R.G. Forbes, J. Vac. Sci. Technol. B **17**, 526 (1999).

Figure Legends

FIG. 1. **SEM images of an H-shaped structure milled in a bilayered $Pd_{80}Si_{20}$ (200 nm)/SiO_2 (500 nm)/Si sample**: (a) before irradiation. (b) after irradiation with 1×10^{16} ions/cm^2 at RT. (c) same as in (b) but after etching in HF for 4 minutes. (d) after etching and an additional irradiation with 1×10^{16} ions/cm^2 at ~80 K. The original FIB milled depth and gap size are ~1.1 μm and ~800 nm, respectively. The sketch at the top is a schematic cross section of the sample.

FIG. 2. **Comparison of width change of each gap of SiO_2 and $Pd_{80}Si_{20}$ in the bilayered structure as a function of ion fluence for irradiations at RT and at 80 K**. The line is a guide for the eyes.

FIG. 3. **(a) Schematic diagram of the two electrodes**. SEM images of the electrodes: (b) before irradiation and (c) after irradiation with 5.65×10^{15} ions/cm^2 at RT.

FIG. 4. **Fluence dependence of the I-V characteristics at RT.** The I-V curve measured after irradiation with 5.65×10^{15} ions/cm^2 is shown in a different horizontal scale. Dashed lines are obtained by a least-squares fit to Equation (1). The best-fit gap distance corresponding to each I-V curve is as follows: ◆:0.006 nm, ◇: 1.8 nm, ▼: 3.0 nm, ▽: 4.2 nm, ■: 5.4 nm, □: 6.5 nm, ▲: 8.3 nm, △: 8.5 nm.

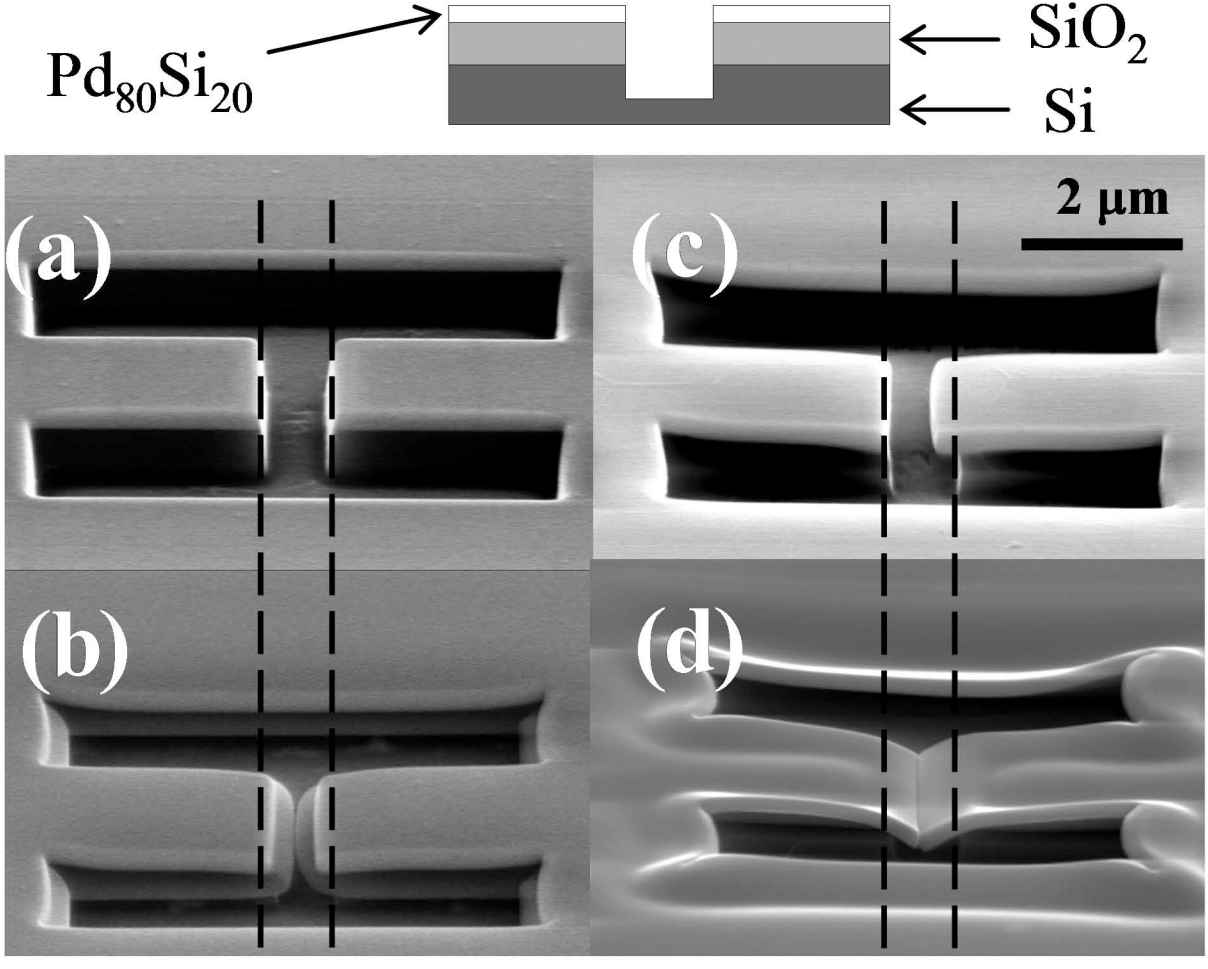
$Pd_{80}Si_{20}$
SiO_2
Si
(a)
(b)
(c)
(d)
2 μm

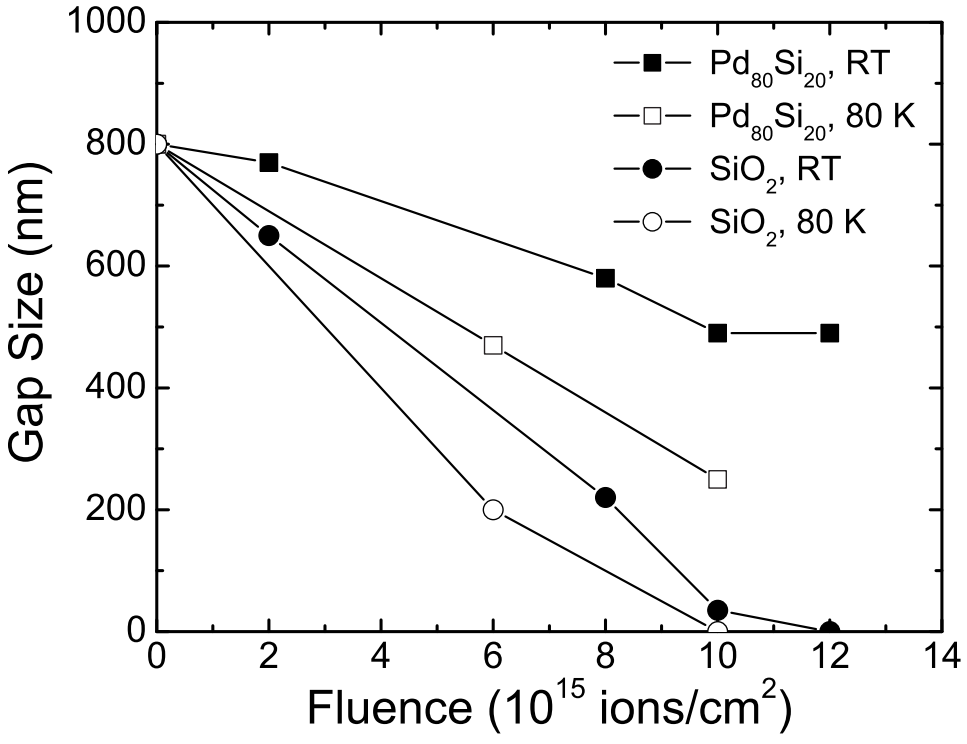
Gap Size (nm)
Fluence (10^{15} ions/cm^2)
$Pd_{80}Si_{20}$, RT
$Pd_{80}Si_{20}$, 80 K
SiO_2, RT
SiO_2, 80 K
0
200
400
600
800
1000
0
2
4
6
8
10
12
14

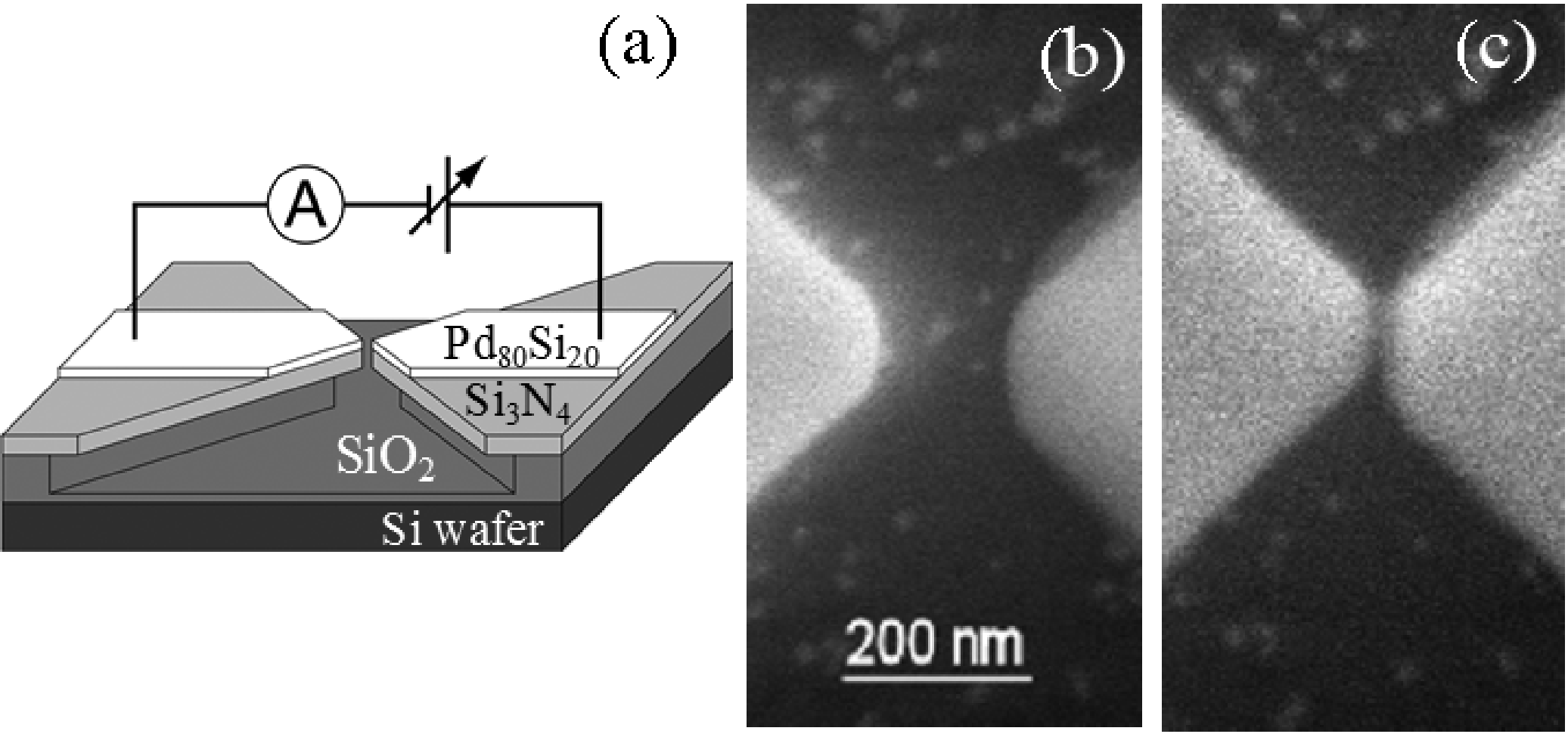
(a)
A
$Pd_{80}Si_{20}$
Si_3N_4
SiO_2
Si wafer
(b)
200 nm
(c)

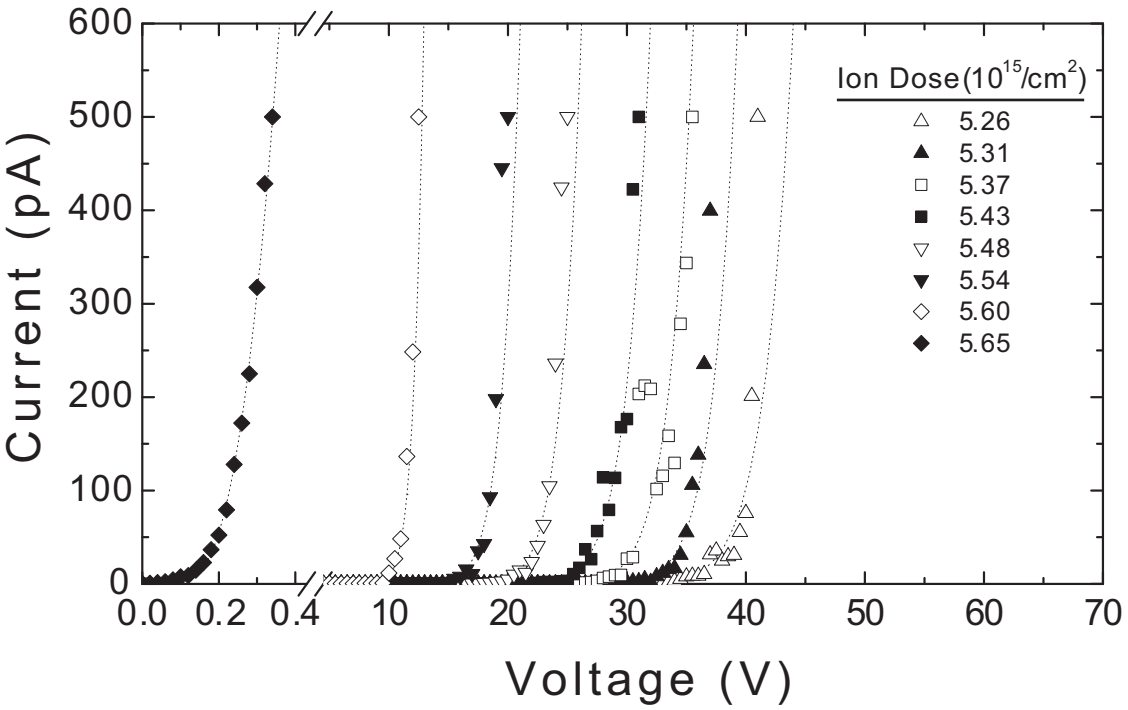
Current (pA)
Voltage (V)
Ion Dose(10^15/cm^2)
5.26
5.31
5.37
5.43
5.48
5.54
5.60
5.65
0
100
200
300
400
500
600
0.0
0.2
0.4
10
20
30
40
50
60
70